



Evaluating the Ability of CRCM5 to Simulate Mixed Precipitation

É. Bresson, R. Laprise, D. Paquin, J.M. Thériault & R. de Elía

To cite this article: É. Bresson, R. Laprise, D. Paquin, J.M. Thériault & R. de Elía (2017) Evaluating the Ability of CRCM5 to Simulate Mixed Precipitation, Atmosphere-Ocean, 55:2, 79-93, DOI: [10.1080/07055900.2017.1310084](https://doi.org/10.1080/07055900.2017.1310084)

To link to this article: <http://dx.doi.org/10.1080/07055900.2017.1310084>



© 2017 The Author(s). Published by Informa UK Limited, trading as Taylor & Francis Group



Published online: 03 May 2017.



Submit your article to this journal [↗](#)



Article views: 316



View related articles [↗](#)



View Crossmark data [↗](#)

Evaluating the Ability of CRCM5 to Simulate Mixed Precipitation

É. Bresson ^{1,2,*}, R. Laprise¹, D. Paquin ², J.M. Thériault¹, and R. de Elía^{1,2,†}

¹Centre pour l'étude et la simulation du climat à l'échelle régionale (ESCER), Université du Québec à Montréal, Montréal, Quebec, Canada

²Ouranos Consortium, Montréal, Quebec, Canada

[Original manuscript received 4 July 2016; accepted 14 February 2017]

ABSTRACT *Precipitation episodes in the form of freezing rain and ice pellets represent natural hazards affecting eastern Canada during the cold season. These types of precipitation mainly occur in the St. Lawrence River valley and the Atlantic provinces of Canada. This study aims to evaluate the ability of the fifth-generation Canadian Regional Climate Model (CRCM5), using a 0.11° horizontal grid mesh, to hindcast mixed precipitation when driven by reanalyses produced by the European Centre for Medium-range Weather Forecasts (ERA-Interim) for a 35-year period. In general, the CRCM5 simulation slightly overestimates the occurrence of freezing rain, but the geographical distribution is well reproduced. The duration of freezing rain events and accompanying surface winds in the Montréal region are reproduced by CRCM5. A case study is performed for an especially catastrophic freezing-rain event in January 1998; the model succeeds in simulating the intensity and duration of the episode, as well as the propitious meteorological environment. Overall, the model is also able to reproduce the climatology and a specific event of freezing rain and ice pellets.*

RÉSUMÉ [Traduit par la rédaction] *Les épisodes de précipitations verglaçantes et de grésil représentent un danger naturel qui touche l'est du Canada durant la saison froide. Ces types de précipitations surviennent surtout dans la vallée du fleuve Saint-Laurent et dans les provinces atlantiques du Canada. Cette étude vise à évaluer la capacité de la 5e génération du Modèle régional canadien du climat (MRCC5), doté d'une maille horizontale de 0,11°, à prévoir a posteriori un mélange de précipitations, quand le modèle est piloté par les réanalyses du Centre européen pour les prévisions météorologiques à moyen terme (ERA-Interim), sur une période de 35 ans. En général, la simulation du MRCC5 surestime faiblement l'occurrence de pluie verglaçante, mais en génère une répartition géographique adéquate. Le MRCC5 reproduit la durée de la pluie verglaçante et les vents de surface associés, dans la région de Montréal. Dans une simulation du cas particulièrement catastrophique de pluie verglaçante de janvier 1998, le modèle a réussi à reproduire l'intensité et la durée de l'épisode, ainsi que l'environnement météorologique sous-jacent. Dans l'ensemble, le modèle peut reproduire tant la climatology qu'un cas précis de pluie verglaçante et de grésil.*

KEYWORDS regional climate model; mixed precipitation; freezing rain; ice pellets; high-resolution; eastern Canada

1 Introduction

During the cold season, freezing rain (ZR) and ice pellets (IP), or a combination of these (hereafter IPZR) can occur in eastern Canada, affecting particularly the St. Lawrence River Valley (SLRV) and the Atlantic provinces (e.g., Cortinas, Bernstein, Robbins, & Strapp, 2004; Groisman et al., 2016; Stuart & Isaac, 1999). The occurrence of ZR results in a layer of ice forming on surfaces, such as roads, sidewalks, trees, and electrical wires, with significant consequences for human activity, infrastructure, and the environment. Numerous occurrences have been reported of injuries caused by car accidents, slippery sidewalks, ruptured cables due to ice accumulation,

and broken tree branches (e.g., Cortinas et al., 2004; DeGatano, 2000; McKay & Thompson, 1969). Statistics from observations show that most of the ZR events last less than four hours (Cheng et al., 2004; Henson & Stewart, 2007; Ressler, Milrad, Atallah, & Gyakum, 2012), but longer episodes also occur, such as the 1998 Ice Storm. This exceptionally long and intense freezing rain event produced ice accumulations up to 100 mm and had catastrophic repercussions in some regions of northeastern North America, with power outages lasting three consecutive weeks in some places around Montréal, Quebec, Canada (e.g., Milton & Bourque, 1999; Regan, 1998; Roebber & Gyakum, 2003).

*Corresponding author's email: emilie.bresson@gmail.com

†Current affiliation: Gerencia de Investigación, Desarrollo y Capacitación Servicio Meteorológico Nacional, Argentina

The occurrence of IP is less frequent and has fewer consequences than ZR events, but both types of precipitation have similar formation mechanisms. In cold-climate conditions, precipitation usually forms aloft in frozen form. When such precipitation falls through a warm air layer with a temperature above freezing, the solid particle melts or partially melts before reaching the cold air layer below. If the particle totally melts in the warm air layer it becomes super-cooled in the cold air layer below and freezes on contact with a surface with a temperature below freezing, leading to ZR (e.g., Thériault & Stewart, 2010; Zerr, 1997). A particle with some remaining ice will initiate freezing in this cold air layer leading to IP. In both cases, the resulting precipitation type differs substantially from the original snowflake shape. The vertical profile of temperature is thus paramount to the discrimination of precipitation types; slight variations in temperature can cause changes in dominant precipitation type (Thériault, Stewart, & Henson, 2010).

In the context of climate change, modifications of precipitation, temperature, and weather patterns could lead to changes in the location, frequency, and intensity of ZR and IP events. Understanding these possible changes is essential to adapting to, and planning for, future conditions in several sectors such as electrical supply, agriculture, and urban infrastructure. Some studies have already estimated the modification of ZR behaviour with climate change using global climate and/or statistical models. They suggest that in the future, more ZR events may occur in higher latitudes and fewer in lower latitudes (e.g., Cheng, Auld, Li, Klaasen, & Li, 2007; Cheng et al., 2004; Klima & Morgan, 2015; Lambert & Hansen, 2011). Although the coarse resolution of global models may be sufficient to simulate large-scale geographical variations of mixed precipitation, it is inadequate for representing the regional details of anticipated future changes. In particular, events that are closely related to fine-scale topography are unseen by global models (Lambert & Hansen, 2011). Regional climate models (RCM) with their finer horizontal grid offer advantageous perspectives for studying the evolution of IP and ZR occurrence in a future climate.

This study aims to evaluate the fifth-generation of the Canadian RCM (CRCM5), which participated in the international Coordinated Regional Climate Downscaling Experiment (CORDEX) for North America (Martynov et al., 2013; Šeparović et al., 2013), to hindcast climate features of ZR and IP events. This is an essential step before attempting climate change projections for ZR and IP species. A CRCM5 simulation was performed with a horizontal grid of 0.11° , which has been documented (Lucas-Picher, Laprise, & Winger, 2016) to be essential for good reproduction of local topographic features, such as the SLRV, where the channelling in the valley can maintain or enhance the cold layer near the surface (Carrera, Gyakum, & Lin, 2009; Razy, Milrad, Atallah, & Gyakum, 2012; Roebber & Gyakum, 2003).

Evaluation of the CRCM5 skill will proceed in two streams. First, the simulated ZR and IP characteristics in terms of

frequency, duration, and specific environment, such as surface wind and vertical temperature profiles, will be analyzed for a 35-year hindcast simulation. Then the severe-storm event of January 1998 will be used to investigate the skill of the CRCM5 in reproducing the appropriate environment, duration, and accumulation for this specific case.

The paper is organized as follows. Section 2 is devoted to a description of the model, the simulation design, the verifying observational data, and the evaluation methodology. The results are presented first for a climatological assessment (Section 3.a) and then for a specific case study (Section 3.b). Conclusions are presented in Section 4.

2 Experimental set-up and data

a Brief Description of CRCM5

The CRCM5 is the fifth-generation Canadian RCM (Martynov et al., 2013; Šeparović et al., 2013) developed by the Centre pour l'étude et la simulation du climat à l'échelle régionale (ESCLER) at the Université du Québec à Montréal (UQÀM). It is based on the limited-area version of the numerical weather-prediction Global Environmental Multi-scale (GEM) model (Côté et al., 1998; Yeh et al., 2002) developed by Environment and Climate Change Canada. The GEM model is a grid-point model based on a two-time-level semi-Lagrangian, (quasi) fully implicit time-discretization scheme. Vertical resolution is defined by a terrain-following vertical coordinate based on hydrostatic pressure (Laprise, 1992). The horizontal discretization is described on a rotated latitude-longitude, Arakawa C-grid (Arakawa & Lamb, 1977). The nesting technique derives from Davies (1976) and consists of a 10-point sponge zone for a gradual relaxation of all the prognostic atmospheric variables toward the driving date along the lateral boundaries with an additional 10-point wide halo zone for semi-Lagrangian interpolation.

Physical parameterizations include the following modules: correlated-K solar and terrestrial radiation (Li & Barker, 2005); subgrid-scale orographic gravity-wave drag (McFarlane, 1987); low-level orographic blocking parametrization (Zadra, Roch, Laroche, & Charron, 2003); planetary boundary layer parametrization (Benoit, Côté, & Mailhot, 1989; Delage, 1997; Delage & Girard, 1992) modified by Zadra et al. (2014) and McTaggart-Cowan and Zadra (2015) to introduce hysteresis effects; the one-dimensional freshwater lake model (FLake; Martynov et al., 2013); and the Canadian Land Surface Scheme, version 3.5 (CLASS3.5; Verseghy, 1991, 2009). The Sundquist (1978) scheme is used as the condensation scheme to diagnose large-scale precipitation. The Kuo-transient scheme is used for shallow convection (Bélair, Mailhot, Girard, & Vaillancourt, 2005; Kuo, 1965). The Kain and Fritsch (1990) scheme is used for deep convection, and total (i.e., large-scale and convective) precipitation is divided into liquid and solid contributions. In addition, surface precipitation types are diagnosed by the Bourguoin (2000) scheme, as described in Section 2.c.

b Experimental Design

The free domain is a 300×300 point grid encompassing northeastern North America (Fig. 1), with a 0.11° horizontal mesh. The vertical domain is defined with 56 levels between the surface and 10 hPa. The time step is five minutes and simulated fields are archived every three hours. The simulation is driven by the reanalysis at 0.75° available at six hourly intervals produced by the European Centre for Medium-range Weather Forecasts (ERA-Interim) (Dee et al., 2011), interpolated linearly in time at every time step. The hindcast simulation starts at 0000 UTC 1 January 1979 and ends at 0000 UTC 1 January 2015. The first year is discarded from the study to allow for spin-up. No large-scale spectral nudging is applied for this simulation.

c The Bourgoiuin (2000) Scheme

The area method of Bourgoiuin (2000) is used to diagnose the types of precipitation in the model. It is based on the energy available for melting in the warm layer aloft and freezing in the cold layer below. Two parameters are salient for discriminating precipitation type: the vertical profile of temperature and the time it takes for hydrometeors to pass through a layer (the residence time). The latter is dependent on the depth of the layer, the mean vertical motion, and the terminal velocity of the falling hydrometeor (Zerr, 1997). The Bourgoiuin scheme assumes that mean vertical motion and terminal

velocity of particles are constant. An area is calculated as the product of the departure of the mean temperature of a layer from 0°C and its thickness and is used as a predictor for determining precipitation type. Positive area (PA) is the part of the temperature vertical profile where temperature is above 0°C while negative area (NA) corresponds to below-freezing temperatures (Fig. 2). To define criteria for discriminating various types of precipitation reaching the surface, the scheme was calibrated by Bourgoiuin (2000) with two sets of observations—collocated surface precipitation and upper-air sounding data—from the 1989/90 and 1990/91 cold seasons over North America. An independent set of observations for 1991/92 was used for validation. Three cases are defined:

- Case A: if $NA < 46 + 0.66PA$: freezing rain,
- Case B: if $46 + 0.66PA \leq NA \leq 66 + 0.66PA$: freezing rain and/or ice pellets,
- Case C: if $NA > 66 + 0.66PA$: ice pellets.

For case B, each species can occur equally, thus precipitation is considered to comprise 50% ZR and 50% IP. As a consequence, ZR and IP can occur at the same time. The Sundquist scheme provides a precipitation rate average archived at three hourly intervals in CRCM5, and this rate is converted into an accumulation over three hours.

This method has several limitations. For example, it assumes that ice crystals are present and that heterogeneous

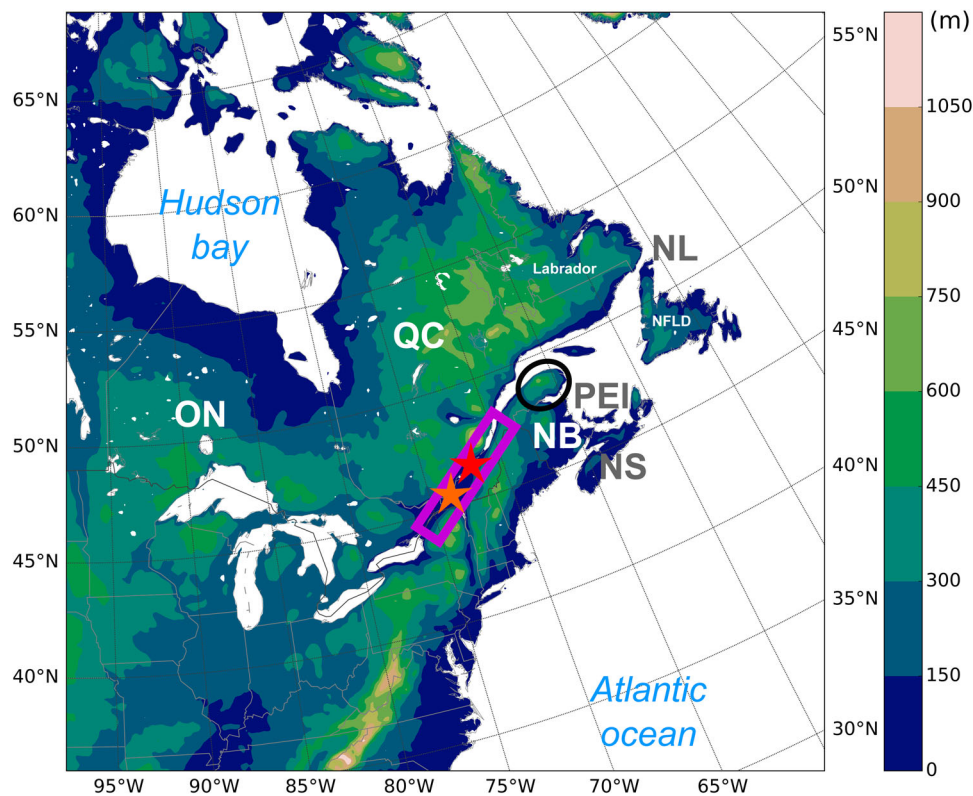


Fig. 1 CRCM5 domain used for this study. Topography (m) is shown in colour. Montréal is shown by the orange star, Québec City by the red star, the St. Lawrence River Valley (SLRV) by the pink rectangle and the Gaspé Peninsula by the black circle. Eastern Canadian provinces are identified as Quebec (QC), New Brunswick (NB), Newfoundland (NFLD) and Labrador (NL), Nova Scotia (NS), Ontario (ON), and Prince Edward Island (PEI).

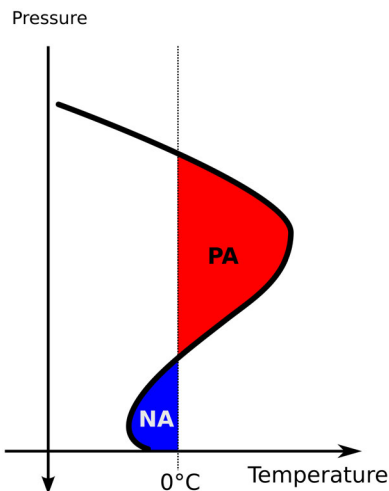


Fig. 2 Schematic of a typical vertical temperature profile for ZR and IP precipitation. The area between the 0°C isotherm and the ambient temperature profile is named the Positive Area (PA; red) when temperature is above 0°C and the Negative Area (NA; blue) when temperature is below 0°C (adapted from Bourgoïn (2000) by permission of the American Meteorological Society).

nucleation has occurred, which can lead to erroneous precipitation type. It neglects the effects of moisture subsaturation. The assumption of a constant terminal velocity is also a weakness because different crystal structures fall at different speeds. Hence, particle-size distribution, as well as the interaction among precipitation types as they fall through the atmosphere, are not considered. In addition, when snow melts in the warm layer and when liquid precipitation freezes upon contact with the frozen ground, the latent heat exchanges are not taken into account as discussed by Lackmann, Keeter, Lee, and Ek (2002). This process could play an important role in reducing the duration of a ZR episode because of surface temperature rising to values above 0°C. A detailed microphysical scheme could avoid these drawbacks but would be much more computationally expensive and require finer horizontal resolution. This is outside the scope of the present study.

d Observational Data

The Meteorological Service of Canada (MSC) of Environment and Climate Change Canada (ECCC) is responsible for surface meteorological stations as outlined in Environment Canada (2015). The frequency of surface weather observations has changed over time and varies by station: it can be hourly; hourly during daytime only; every three hours; or every six hours. Some stations have records of variables such as 2 m temperature, 2 m dew point temperature, 2 m relative humidity, 10 m wind direction and speed, visibility, atmospheric surface pressure, and reports that distinguish between the different types of precipitation: liquid precipitation (drizzle and rain), freezing precipitation (freezing

drizzle and ZR), frozen precipitation (snow, snow pellets, snow grains, IP, hail, and ice crystals) and other hydrometeorological deposits, such as dew, hoar frost, rime, and glaze. In this study, we focus on ZR, IP, and 10 m wind data from the hourly observations at surface stations in the Canadian provinces of Quebec (QC), Ontario (ON), Newfoundland and Labrador (NL), Prince Edward Island (PEI), Nova Scotia (NS), and New Brunswick (NB). In all, 77 surface stations provided daily ZR and IP data for at least one year during the study period, as indicated by the blue crosses in Fig. 3. It was decided, however, to retain only stations with at least 30 years of available data within the 35-year period, which results in a set of 48 surface stations, as indicated by the grey circles in Fig. 3. Montréal's Pierre Elliott Trudeau International Airport surface station (hereafter YUL), indicated by the orange star in Fig. 1 and the red circle in Fig. 3, provides observations until mid-February 2013 only; thus for the Montréal region, the study considers only the period from 1980 to 2012.

Hourly records from ECCC surface weather stations provide an estimate of ZR intensity, as light (2.5 mm h^{-1} or less), moderate (2.6 to 7.5 mm h^{-1}) and heavy (7.6 mm h^{-1} or more) intensities. Hence, for our climatological study, we will focus on the occurrence of ZR rather than ZR amount. A precise measurement of ZR amount can be obtained by melting ice accumulated in the rain gauge and measuring the water equivalent. For example, Milton and Bourque (1999) used data from about 130 surface stations in the MSC network between 0600 UTC 4 January and 0600 UTC 10 January 1998 to characterize the intensity of the 1998 Ice Storm (Fig. 4). Because of their shape and rigidity, IPs tend to rebound after touching most surfaces, and this causes some difficulty for a precise measurement with rain gauges; the IP precipitation intensity is thus only defined as light, moderate, or heavy.

e Methodology for Event Identification

The ZR and IP episodes are determined when precipitation intensity exceeds a threshold. In the hourly observation dataset, precipitation rate is recorded when a measurement above 0.2 mm h^{-1} is registered, whereas it is recorded simply as a trace if the rate is below this threshold. On the other hand, the CRCM5 precipitation archive available to us is the three-hour cumulative amount. Also, as is the case for most models, the CRCM5 tends to produce excessive light precipitation events (Biner, 2016). For these reasons, we decided to use a threshold of 1 mm d^{-1} (i.e., about 0.04 mm h^{-1}), as did Lambert and Hansen (2011). When this threshold is reached, three hours of simulated precipitation are recorded. For consistency, hourly observations are aggregated in three-hour periods and for each block of three-hour data, one or more hours of occurrence is reported as three hours of occurrence. Finally, the duration of an event is defined as the cumulative time between the first and last

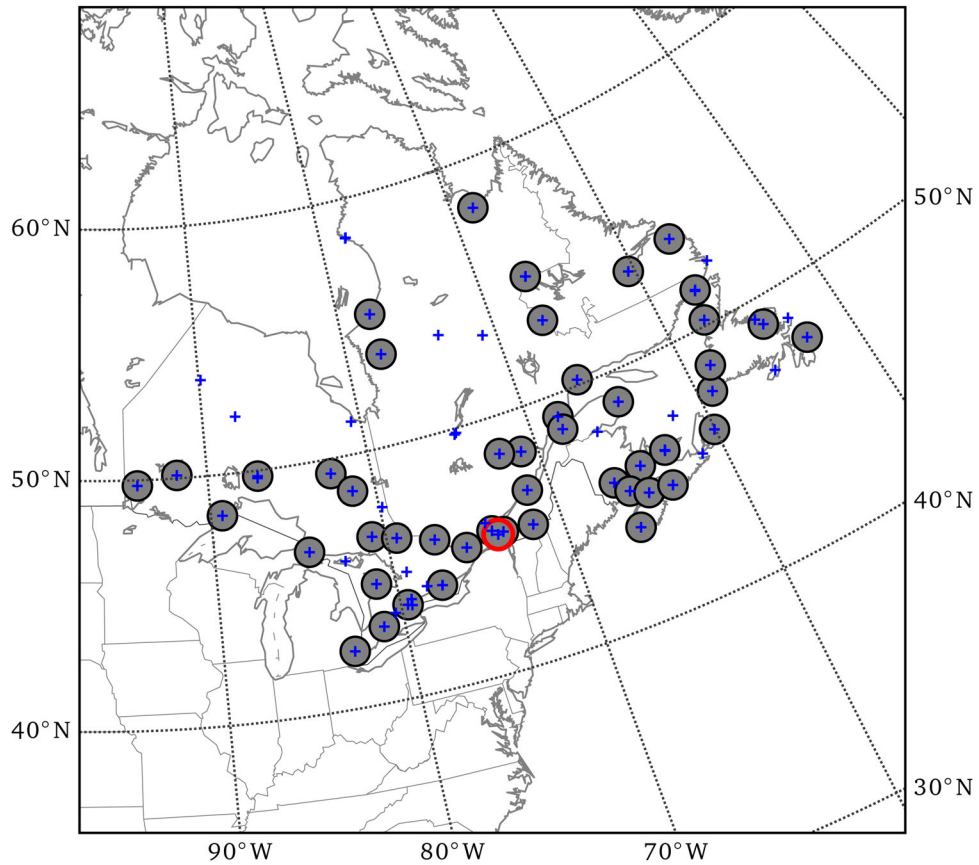


Fig. 3 Crosses indicate the locations of surface stations with hourly data available all day long for at least one year within the 1980–2014 period; the grey filled circles correspond to stations with data available for 30 consecutive years within the 1980–2014 period. Montréal’s Pierre Elliott Trudeau International Airport station is indicated with a grey and red circle.

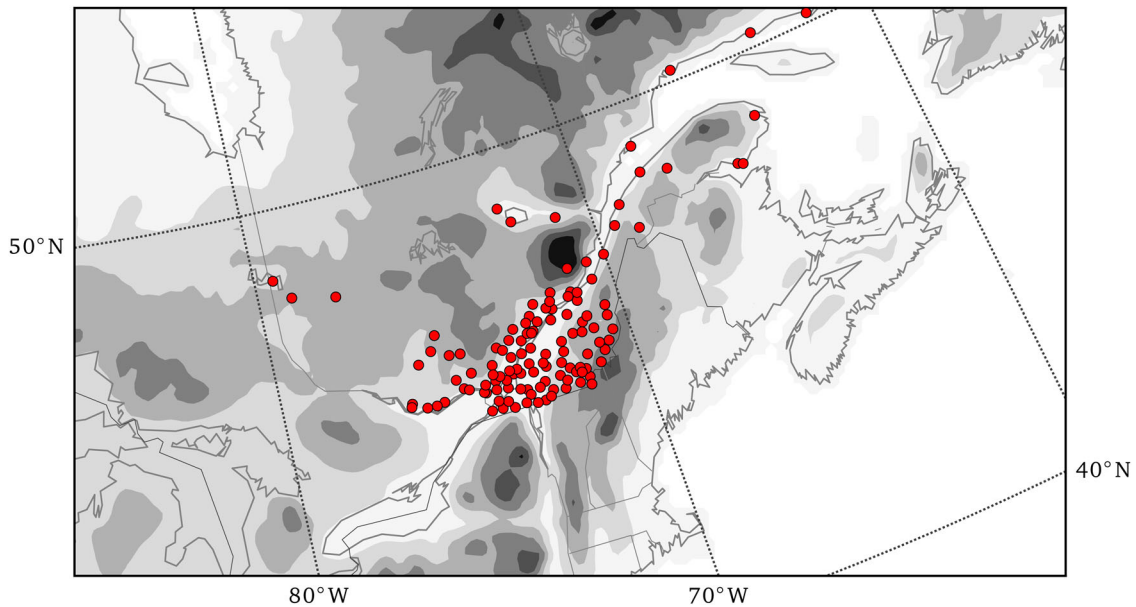


Fig. 4 Location of surface stations available for accumulation measurement of ZR between 0600 UTC 4 January 1998 and 0600 UTC 10 January 1998, superposed on CRCM5 topography (grey tones).

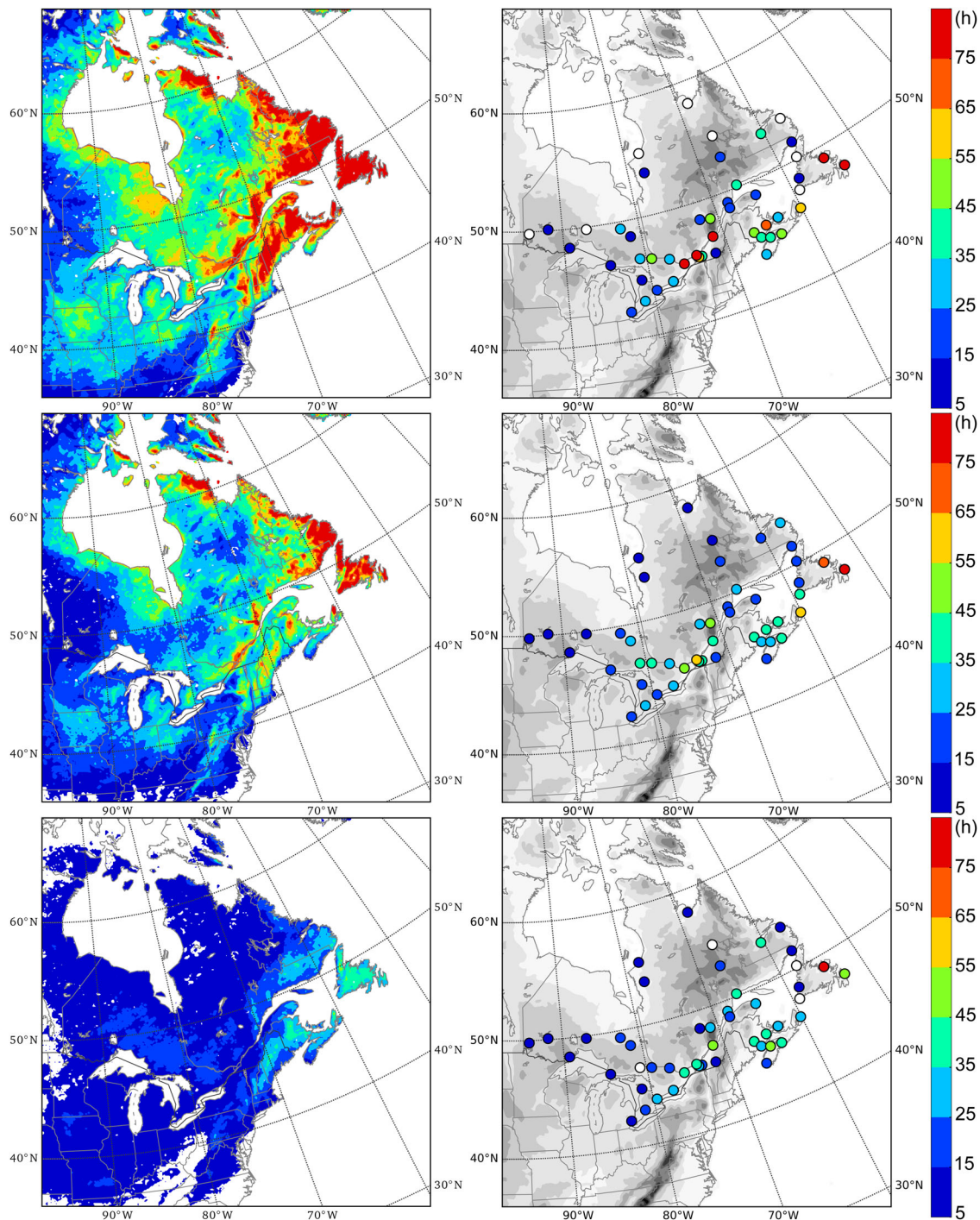


Fig. 5 Median of annual hours of IPZR (top), ZR (middle), and IP (bottom) simulated by CRCM5 (left) and observed (right) superposed on the CRCM5 topography (grey tones) for 1980–2014.

detection of ZR and/or IP occurrence, allowing up to six hours without precipitation in order to avoid counting too many very short events, as in the study of Ressler et al. (2012).

Some standard statistical indicators are used for the evaluation of the CRCM5 performance: bias, root mean square error (RMSE), and a least square regression (LSR). To compare a particular simulated parameter with an observation, for each of the observation locations, the nearest model grid

point and surrounding eight points are selected; the parameter value is then averaged on the grid points within this selection only if their percentage of land is larger than 75%. The sensitivity to the number of points selected for the comparison between an observation and the model has been explored and small differences were noted. Using a 9-grid-point box is then a good compromise between statistical stability and resolution.

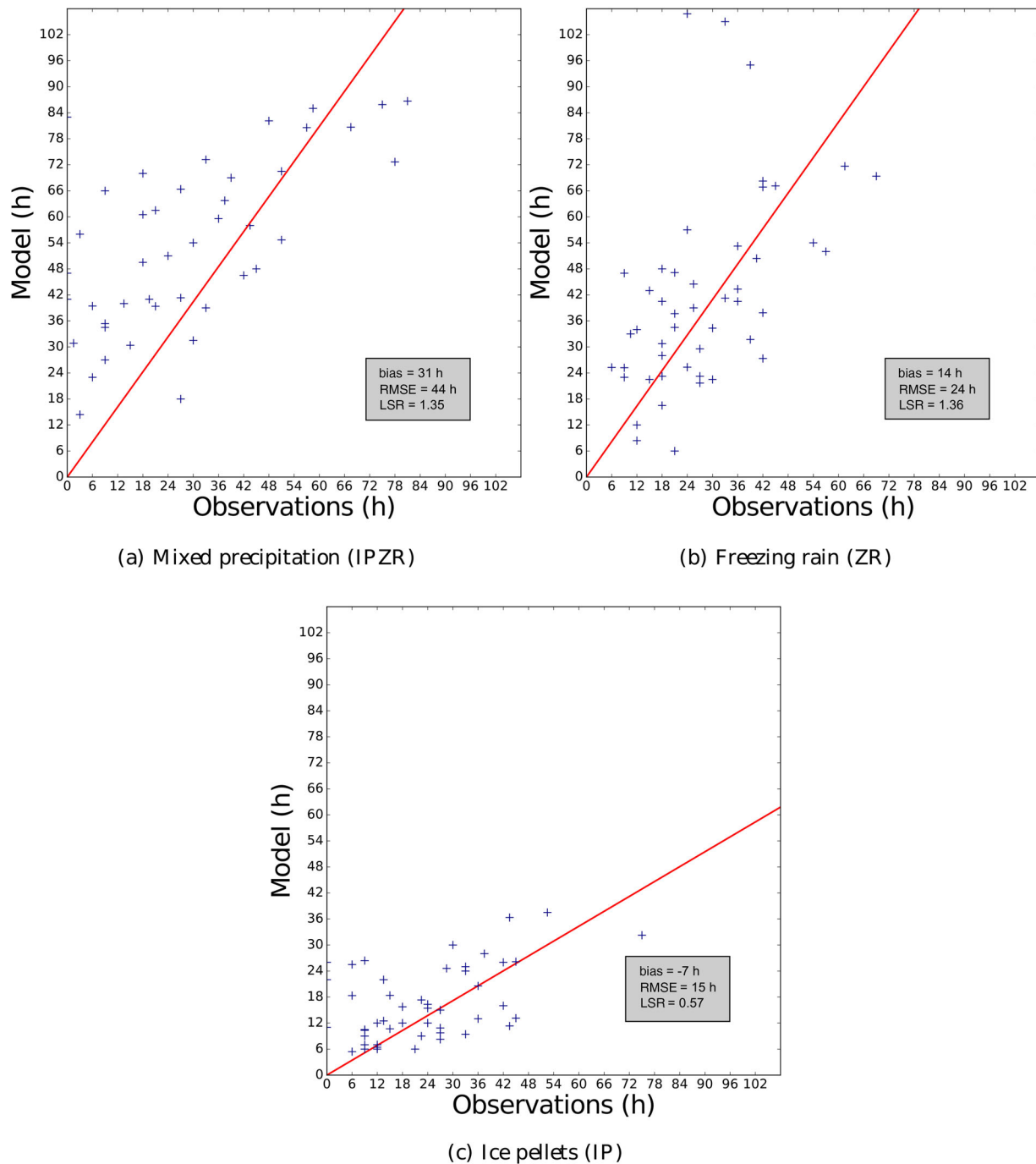


Fig. 6 Scatterplot of median annual hours observed and simulated for (a) IPZR, (b) ZR, and (c) IP. Observation values are compared with the average simulated value on the points over land among the nine nearest grid points. The bias, RMSE, and coefficient of LSR are also indicated.

3 Results

This section presents a general description of the observed and simulated climatology of mixed precipitation over eastern Canada. The next subsection presents the climatological pattern of occurrence and associated low-level wind flow over the SLRV. The second subsection describes the favourable meteorological environment and the mechanisms involved in mixed-precipitation formation.

a Climatological Assessment

1 MIXED PRECIPITATION FREQUENCY OVER EASTERN CANADA

The distribution of IPZR mixed precipitation over eastern Canada exhibits high frequencies for the SLRV, Gaspé Peninsula, NB, NS, Newfoundland (NFLD), and northeastern Labrador (Cortinas et al., 2004; Lambert & Hansen, 2011). Figure 5 shows that the CRCM5 simulation succeeds overall

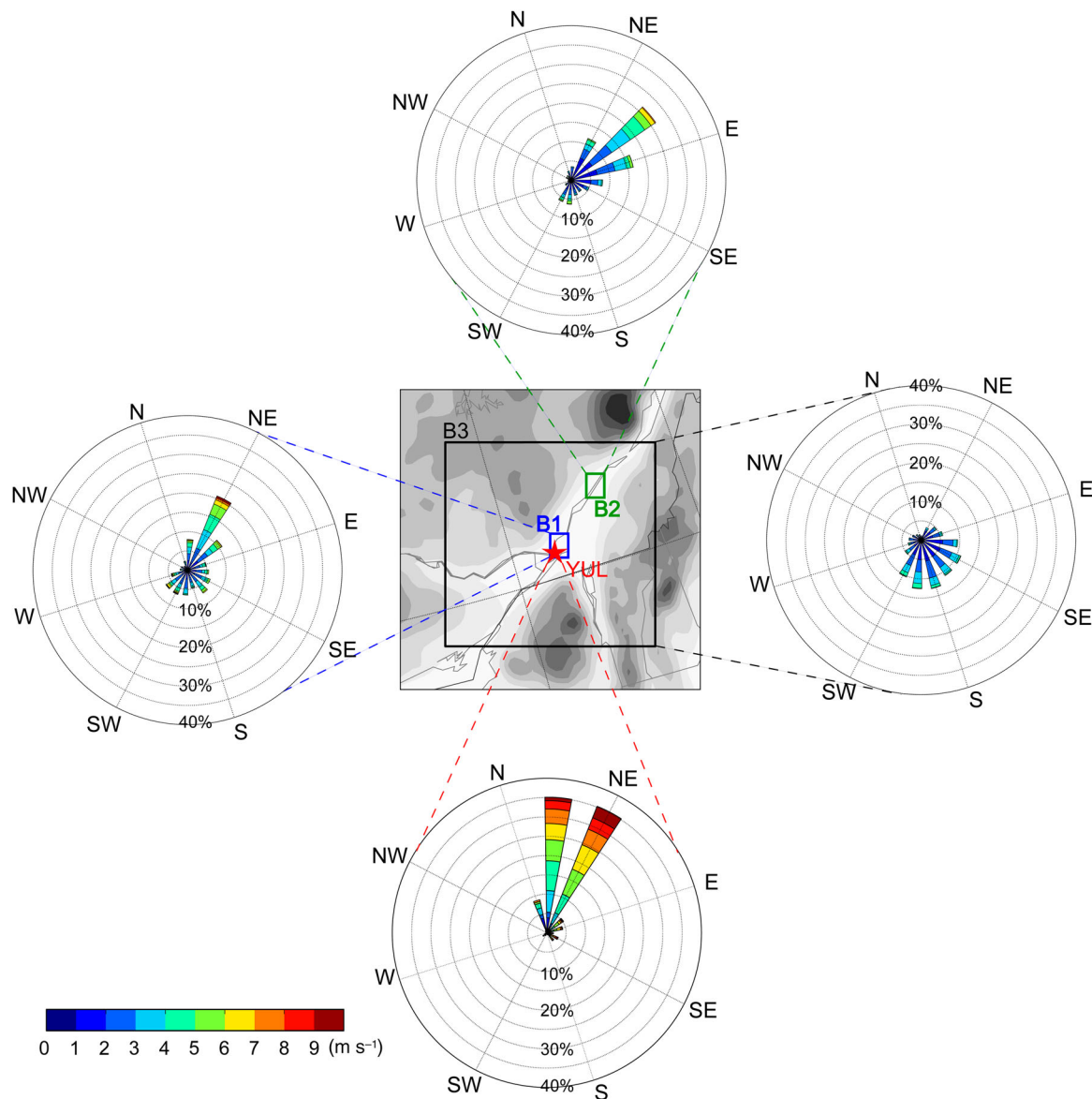


Fig. 7 10 m wind simulated in small 3×4 grid-point boxes near Montréal (B1), near Québec (B2), and over a larger 50×50 grid-point domain (B3) for all ZR events occurring in the B1 domain. The anemometer-level winds observed at YUL during the ZR events between 1980 and 2012 are also shown. Wind intensities (m s^{-1}) are in colour and the percentage of winds for each direction are shown in radial direction.

in reproducing this pattern although with an overestimate of about 35% over the entire domain, with a bias of 31 hours and an RMSE of 44 hours (Fig. 6a). Because IPZR corresponds to the occurrence of IP and/or ZR, the median of IPZR annual hours is not the sum of the same parameters for IP and ZR. Simulated values of IPZR over northern QC and northern Labrador appear more intense compared with available observations, whereas they are comparable in the SLRV. Figure 5 shows that ZR preferentially occurs in the SLRV, NB, NFLD, and northeastern Labrador; ZR is simulated more often in northeastern QC and northern NFLD than in observational data. Compared with the 48 surface stations, the ZR simulated bias and RMSE are smaller than for IPZR (bias = 14 h; RMSE = 24 h), but the 36%

overestimate is similar to the IPZR overestimate (Fig. 6b). Simulated IP is less frequent than ZR (Fig. 5) and appears to be underestimated by about 33% compared with available observations (Fig. 6c). Hence, the CRCM5 simulations using the Bourgouin scheme produced an excess of ZR and a deficit of IP occurrences. The large differences between simulated and observed values of IPZR and ZR over the extreme northeastern part of the domain could be a consequence of (i) the wet bias of the CRCM5 over these regions and/or (ii) the tendency for weather stations in this region to be located in less exposed coastal locations near sea level. Moreover, given the extreme sensitivity of precipitation types to temperature profiles near the freezing point, it is quite likely that the empirical parameters of the Bourgouin

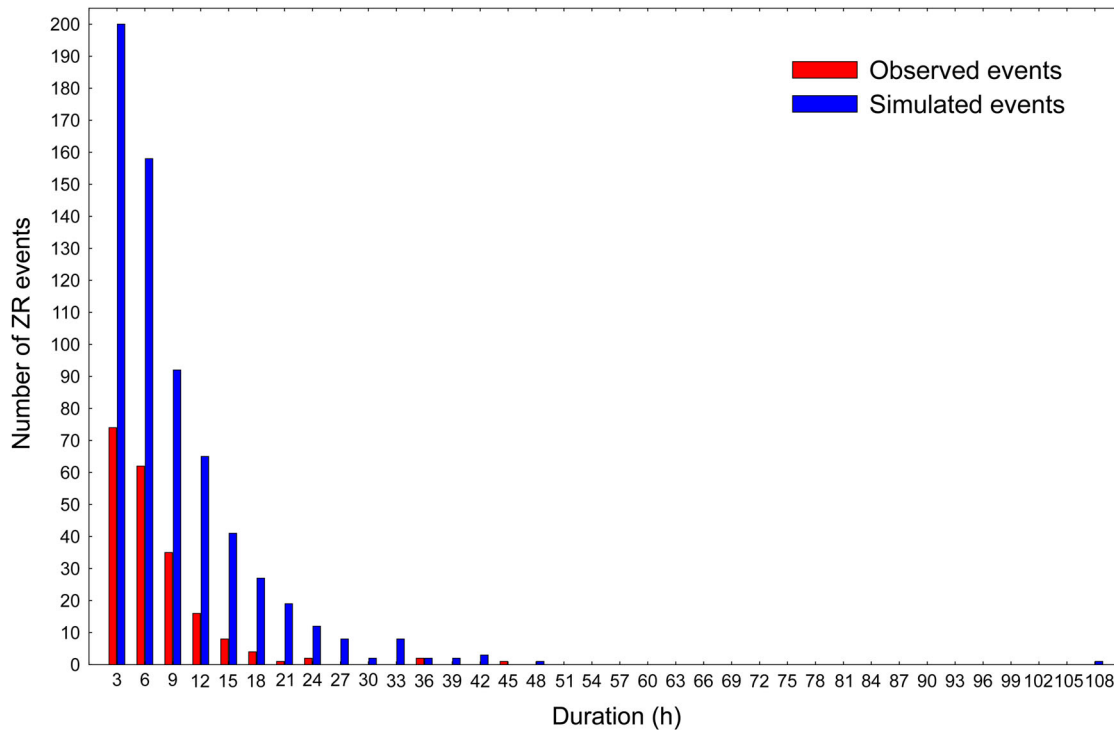


Fig. 8 Histogram of the number of ZR hours per event, in three-hour intervals, observed at the Pierre Elliott Trudeau airport in Montréal (YUL; red) and simulated over the Montréal B1 domain using a threshold of 1 mm d^{-1} (blue) between 1980 and 2012.

scheme could be retuned to optimize the simulated results compared with the available observations, but no attempt was made to do this in this study; the original parameter settings in use at MSC were used.

2 SURFACE WIND IN THE SLRV

The CRCM5 simulated climatology of mixed precipitation using the Bourgouin scheme is encouraging overall. Nevertheless, it is important to ensure that the good agreement between model and observations results from the correct physical processes, especially as far as mesoscale processes are concerned. For example, wind channelling within the SLRV can often lead to intense low-level cold-air advection keeping the surface temperature below freezing when an approaching warm front brings warm-air advection aloft. Previous studies (Carrera et al., 2009; Razy et al., 2012) documented the preponderance of northeasterly to north-northeasterly surface winds during ZR events in the SLRV.

The hourly observations of 10 m wind at YUL confirm that during occurrences of ZR winds are, by and large, north-northeasterly and northeasterly (Fig. 7).

Figure 7 also compares the simulated surface winds with observations made during the occurrence of simulated ZR near Montréal. Two small boxes encompassing 3×4 grid points were selected, one near Montréal (B1) and one downstream near Québec (B2). A larger domain centred on Montréal with 50×50 grid points (B3) was also selected. The

surface winds in the B1, B2, and B3 domains were computed in wind roses for each time simulated ZR exceeded 1 mm d^{-1} for at least one grid point in the B1 domain.

In the B1 domain, 47% of simulated winds are from the northeast quadrant, with a prevalence of northeasterly winds (21%), aligned with the SLRV (Fig. 7). Downstream, in the B2 domain, the simulated surface winds are mainly from east-northeast (26%) and east (16%) in the axis of the valley when ZR occurs in the Montréal area (Fig. 7). The B3 box wind rose, on the other hand, conveys the averaged behaviour of larger-scale simulated surface winds; these are quite different from the B1 and B2 wind roses, showing only 17% of surface winds occurring in the northeast quadrant and a larger contribution of southerly winds characteristic of a warm front approach.

In general, a smaller fraction of the simulated surface winds are from the north-northeast and northeast, than found at YUL. One must keep in mind that the observation station is located in the southwest section of Montréal Island. Also, because there is no gust module in CRCM5, simulated surface winds will tend to be weaker than observed ones, which could influence the duration of the simulated ZR events over the Montréal region.

3 DURATION OF ZR EVENTS OVER MONTRÉAL

Because of the transitional environment propitious to their formation, ZR events are characterized by their short durations (e.g., Ressler et al., 2012). The duration of simulated ZR events is calculated on the B1 domain and compared with YUL surface

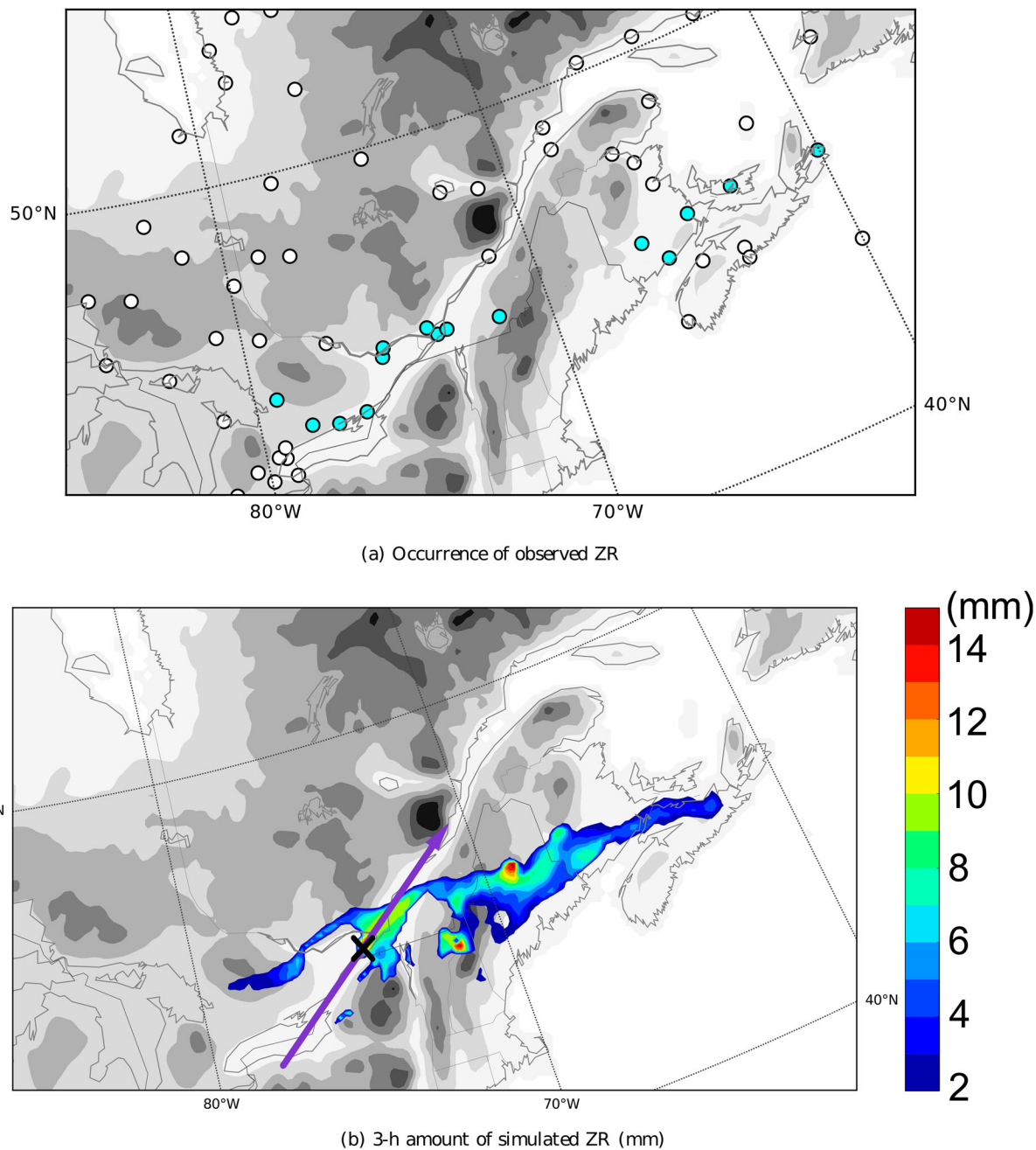


Fig. 9 (a) Occurrence of observed ZR between 1800 UTC and 2100 UTC 8 January 1998: white dots indicate no observed ZR and turquoise dots indicate that ZR was observed. (b) Three-hour amount of ZR (mm) at 2100 UTC 8 January 1998. The cross near Montréal indicates the location of the maximum ZR amount at that time, and the CRCM5 topography is shown in grey shading. The purple line indicates the vertical cross-section presented in Fig. 10.

observations for the 1980–2012 period in Fig. 8. A total of 205 events are recorded for observations and 641 in the CRCM5 simulation. Both simulation and observations exhibit an overall decrease in frequency with duration, with more than 50% of the simulated and observed ZR episodes lasting six hours or less. The large number of simulated events could be due to the moist bias of the CRCM5 and to the choice of a 12-point grid-point box to evaluate simulated ZR.

The 108-hour event in the CRCM5 simulation corresponds to the 1998 Ice Storm. In the observations, this event is

counted as two episodes of 39 and 45 hours linked to the two phases of the 1998 Ice Storm because of the episode criterion of a six-hour maximum without mixed precipitation. This storm will be studied in more detail in the next subsection.

b The 1998 Ice Storm

The 1998 Ice Storm is one of the most catastrophic recorded in history (Institute for Catastrophic Loss Reduction, 2013).

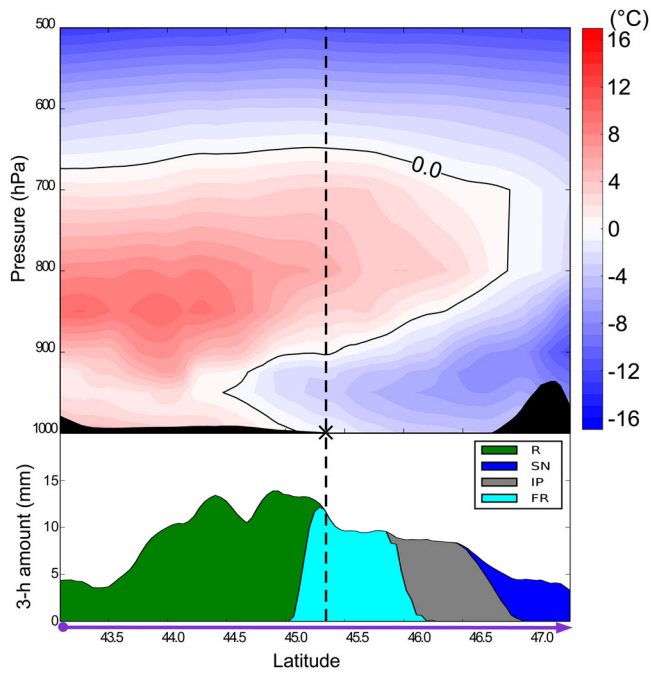


Fig. 10 (top) Vertical cross-section of CRCM5-simulated temperature ($^{\circ}\text{C}$) at 2100 UTC 8 January 1998 along the purple arrow shown in Fig. 9b. (bottom) Simulated three-hour cumulative amounts of ZR, IP, snow (SN), and rain (R) along the purple arrow. The cross corresponds to the location of the maximum ZR amount at that time shown in Fig. 9b.

This storm was characterized by two episodes of mixed precipitation between 0600 UTC 4 January 1998 and 0600 UTC 10 January 1998 (Gyakum & Roebber, 2001; Henson, Stewart, Kochtubajda, & Thériault, 2011; Milton & Bourque, 1999; Roebber & Gyakum, 2003). This extreme event will be investigated to assess the ability of the CRCM5 to realistically reconstruct the favourable environmental conditions.

The CRCM5 simulation is driven by ERA-Interim reanalysis data at its lateral boundaries, but neither large-scale spectral nudging nor data assimilation is used to force the interior of the domain. The use of a relatively small domain, however, ensures that the simulation will follow the observed large-scale atmospheric circulation rather well.

Figure 9a shows observed occurrences of ZR between 1800 and 2100 UTC on 8 January 1998 and Fig. 9b shows simulated three-hour cumulative ZR amount at 2100 UTC on 8 January 1998, corresponding to the time of the most intense simulated ZR during the storm. The observed ZR pattern is reproduced reasonably well by the simulation during this period. The top panel of Fig. 10 shows a vertical cross-section of CRCM5-simulated temperature along the SLRV transect indicated by the purple line in Fig. 9b, and the bottom panel of Fig. 10 shows the intensity of various precipitation types along the same SLRV transect, as diagnosed with the Bourguin scheme. Crosses in Fig. 9b and Fig. 10 indicate, for reference, the location of the maximum simulated ZR intensity,

southwest of Montréal. The bottom panel of Fig. 10 shows that from southwest to northeast, precipitation changes from rain to ZR to IP and finally to snow. This distribution is consistent with the thinning of the warm layer between 700 and 900 hPa and the thickening of the cold tongue in the low levels.

Figure 11 shows the simulated (Fig. 11a) and observed (Fig. 11b) cumulative ZR amount between 0600 UTC 4 January 1998 and 0600 UTC 10 January 1998. The ZR maximum of (110 mm) near Montréal is simulated well although the simulated maximum is displaced somewhat to the west of the maximum in the observations.

Figure 12 shows the time evolution of the intensity of the various precipitation types during the 1998 Ice Storm, as simulated at the grid point indicated by the cross in Fig. 9b. The documented two distinct phases of the storm are well reproduced in the simulation. The hiatus in ZR occurrence during the storm, both in the observations and the simulation, is due to an absence of precipitation while the vertical-temperature structure remained propitious (Milton & Bourque, 1999). The simulated temperature indicates the presence of a warm layer that is too thick and/or too warm to produce IP between 1800 UTC 6 January 1998 and 1800 UTC 9 January 1998, unfortunately, no sounding was available in this area to confirm this point. Figure 12 shows that with time, snow initially present changes to IP and ZR as the mid-altitude warm layer propitious for mixed precipitation establishes itself. Near the end of the storm, the warm air tongue recedes and ZR gives way to IP and eventually to snow.

Some soundings are available to evaluate the vertical structure of the atmosphere, but only the Maniwaki sounding can be used because it is the closest to the area affected by the 1998 Ice Storm (purple square in Fig. 11a). Figure 13 shows the observed and simulated soundings from 0000 UTC 5 January 1998 to 1200 UTC 9 January 1998. The simulated profile is the mean of the temperature profiles of the nearest grid point and the eight grid points surrounding it. The results were similar whether only one grid point or twenty-five grid points were used. A warm tongue is simulated earlier than observed (5 January 1998), and simulated profiles then become quite similar (6 January 1998) but when compared with observations did not last long (1200 UTC 7 January 1998). A simulated temperature profile favouring ZR production suggested a second phase in the experiment but not in the observations. Unfortunately during the event, no precipitation data were available at the Maniwaki station to evaluate the simulated precipitation.

4 Concluding remarks

A hindcast simulation of CRCM5 on a 0.11° mesh driven by ERA-Interim reanalysis data from 1979 to 2014 was carried out to evaluate the ability of the model to reproduce the observed climatology and characteristics of mixed

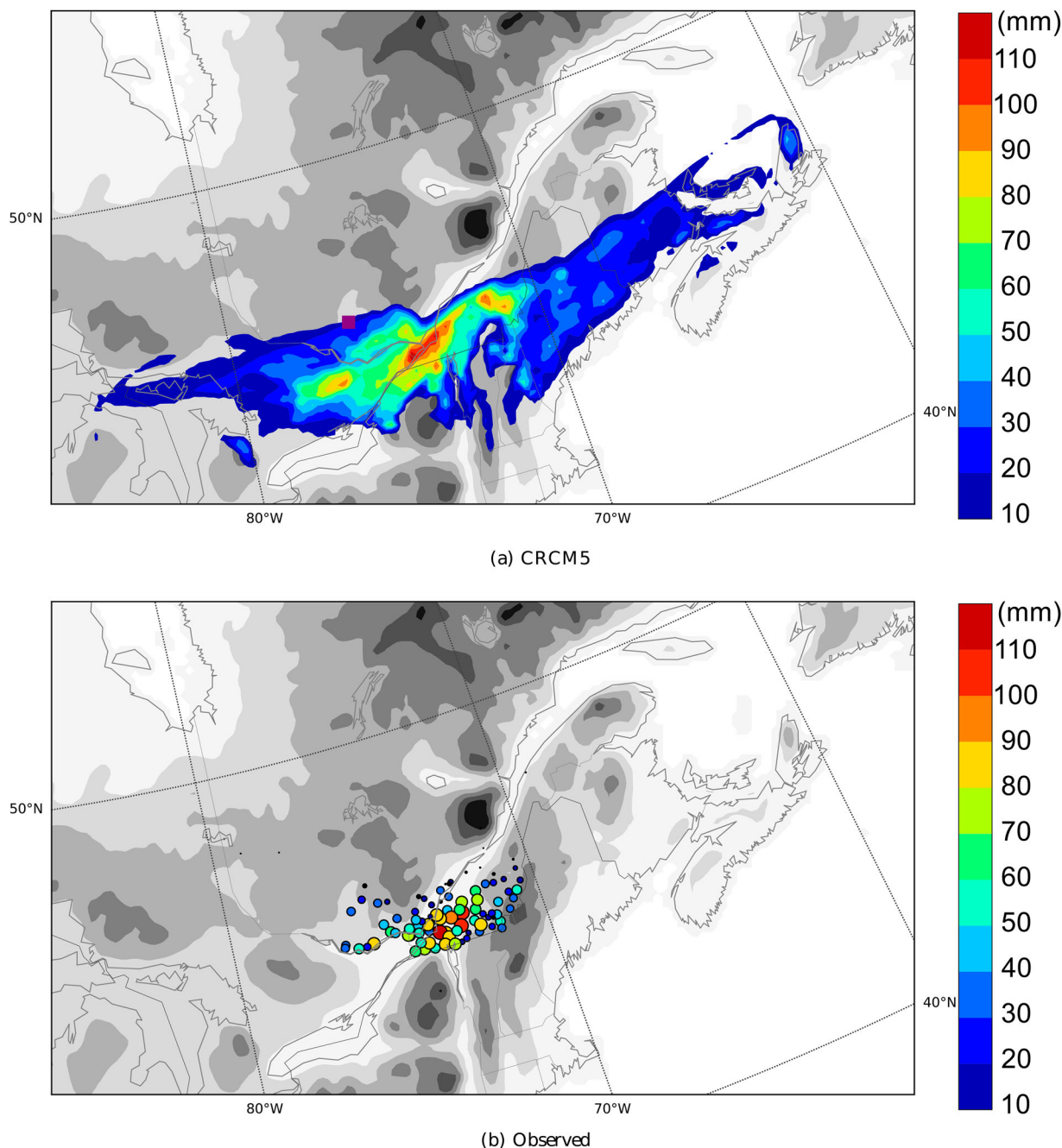


Fig. 11 Cumulative amount of ZR between 0600 UTC 4 January 1998 and 0600 UTC 10 January 1998 (a) simulated by the CRCM5 and (b) observed (taken from data analyzed by Milton & Bourque (1999)). Intensity for observations is represented by both the size of the dots and their colour. The CRCM5 topography is shown in grey shading.

precipitation, especially ZR and IP. The 1998 Ice Storm provided an excellent case study to investigate the CRCM5's capacity to simulate the favourable environmental conditions for such extreme events.

Overall, the model simulated the spatial pattern of mixed-precipitation distribution reasonably well but with a clear tendency to overestimate the number of hours of mixed precipitation (IP and/or ZR) and to underestimate the length of time that only one precipitation type occurred. The simulation

reproduced the climatology of the surface winds during ZR events occurring near Montréal, clearly showing dominant winds in the SLRV with a clear propensity for the northeasterly direction, aligned with the SLRV axis, while concomitant large-scale flow exhibits a dominant southerly flow characteristic of approaching warm fronts. This point is consistent with the particular topography of the region. The simulation also showed comparable duration, intensity, and meteorological environment propitious to ZR and IP formation. The

Evaluating the Ability of CRCM5 to Simulate Mixed Precipitation / 91

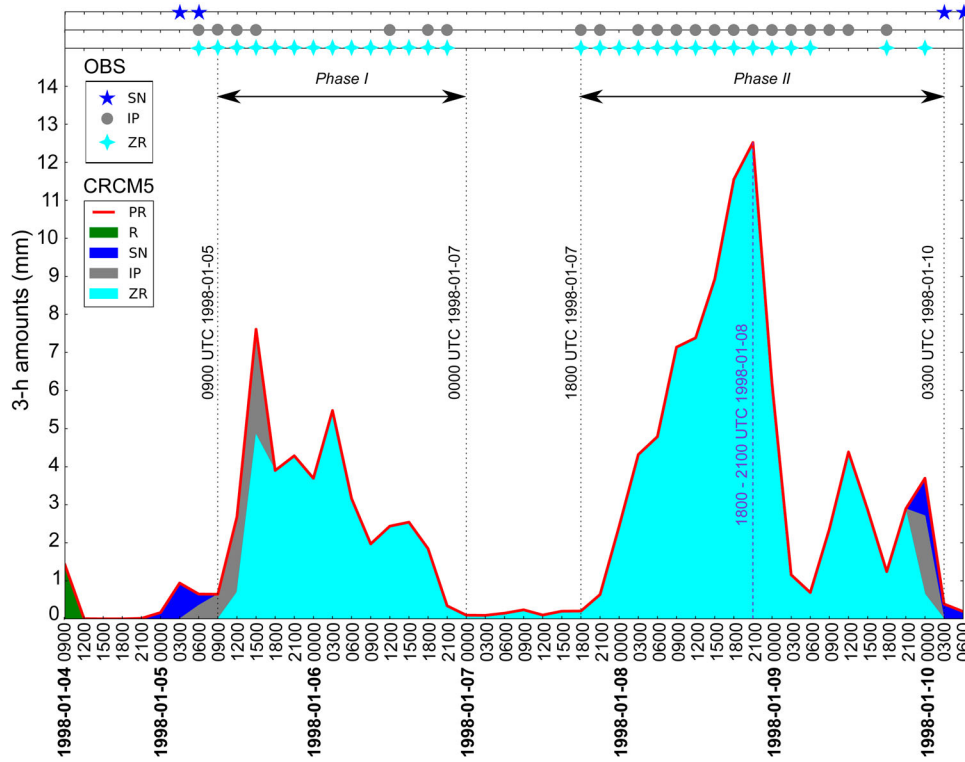


Fig. 12 Time series between 0600 UTC 4 January 1998 and 0600 UTC 10 January 1998 of three-hour cumulative simulated precipitation (mm) in the form of rain (R), snow (SN), ice pellets (IP), freezing rain (ZR), and total precipitation (PR), for the grid point indicated with a black cross in Fig. 9b. Crosses, dots, and stars represent observed occurrences of ZR, IP, and SN, respectively, at Montréal Pierre Elliott Trudeau airport (YUL) for three-hour periods between 0600 UTC 4 January 1998 and 0600 UTC 10 January 1998.

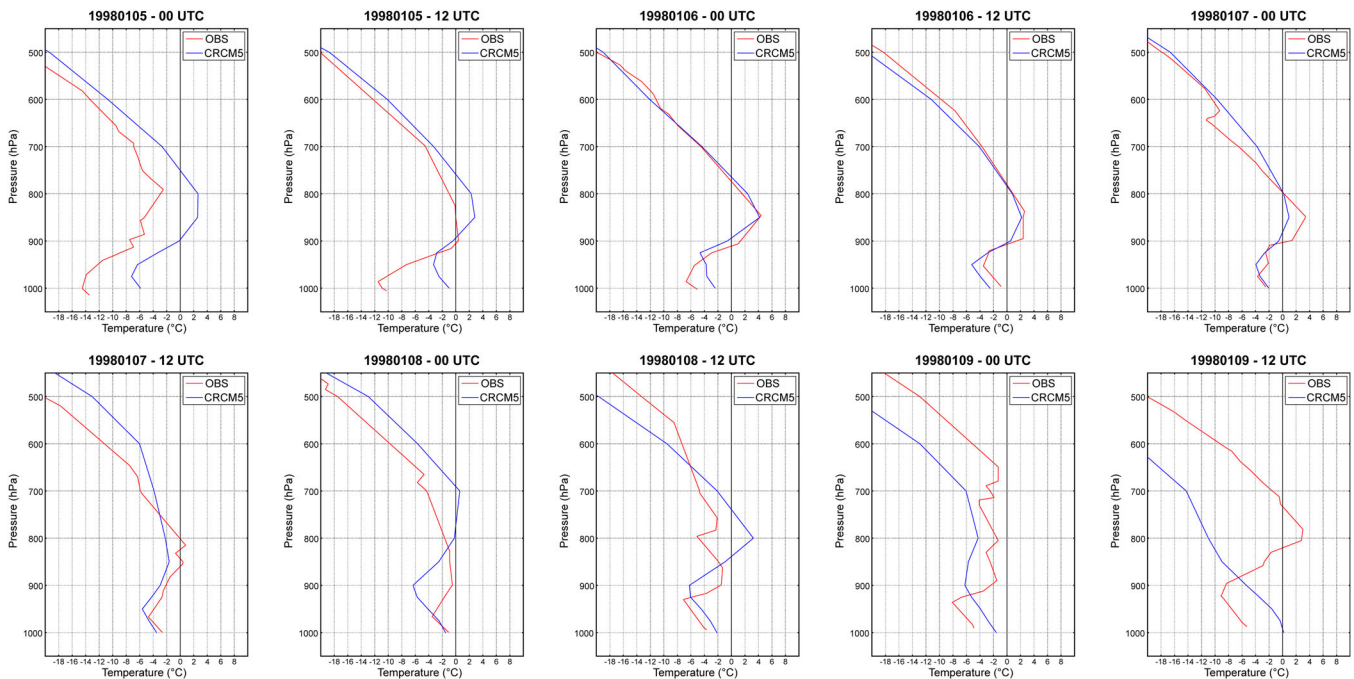


Fig. 13 Maniwaki soundings observed (red) and simulated (blue) by CRCM5. The simulated profile is the mean of temperature for the nearest grid point and the eight grid points surrounding it. The location of Maniwaki is shown in Fig. 11a by a purple square.

simulation also successfully reproduced the two phases of the 1998 Ice Storm.

It is worth noting that the reliability of the surface observations used in this study is often questionable. Despite several procedures applied to these data by responsible authorities, some errors remain almost unavoidable because of either human error or measurement difficulties, which could not have been reported. The empirical Bourgouin scheme has several limitations, as discussed in Section 2.c. Some of these could be removed by the use of a detailed microphysical scheme, which is a topic of current research at the ESCER Centre.

Nevertheless this study provides encouraging results on the ability of CRCM5 to reproduce observed mixed-precipitation characteristics over eastern Canada when driven by reanalysis data. Such a study is a prerequisite to undertaking a projection of changes associated with anticipated global climate changes.

Acknowledgements

The authors want to thank Professor John Gyakum (McGill University) and Mr. Sébastien Biner (Ouranos) for helpful discussions. The authors would like to acknowledge the Data Access Integration (DAI) Team for providing the data and technical support. The DAI Portal is made possible through collaboration among the Canadian Centre for Climate Modelling and Analysis (CCCma), the Division de recherche en prévision numérique (RPN), and the Adaptation and Climate

Monitoring section of ECCC. Thanks to Dr. Éva Mekis and Mylène Gosselin (ECCC) who provided us with useful information about surface stations.

Funding

This work was supported by the Natural Sciences and Engineering Research Council of Canada (NSERC) through a grant to the Canadian Network for Regional Climate and Weather Processes (CNRCWP) [433915-2012], as well as Hydro-Québec Institut de recherche and the Accelerate program of the Network of Centres of Excellence Mitacs [IT06591], and Ouranos. Computations were made on the supercomputer guillimin at McGill University managed by Calcul Québec Compute Canada. The operation of this supercomputer, is funded by the Canada Foundation for Innovation (CFI), the Ministère de l'Économie, de la Science et de l'Innovation du Québec (MESI), and the Fonds de recherche du Québec - Nature et technologies (FRQNT).

Disclosure statement

No potential conflict of interest was reported by the authors.

ORCID

É. Bresson  <http://orcid.org/0000-0002-5289-4937>

D. Paquin  <http://orcid.org/0000-0002-1353-930X>

References

- Arakawa, A., & Lamb, V. R. (1977). Computational design of the basic dynamical processes of the UCLA general circulation model. *Methods in Computational Physics*, 17, 173–265.
- Bélair, S., Mailhot, J., Girard, C., & Vaillancourt, P. (2005). Boundary layer and shallow cumulus clouds in a medium-range forecast of a large-scale weather system. *Monthly Weather Review*, 133(7), 1938–1960.
- Benoit, R., Côté, J., & Mailhot, J. (1989). Inclusion of a TKE boundary layer parameterization in the Canadian regional finite-element model. *Monthly Weather Review*, 117(8), 1726–1750.
- Biner, S. (2016). *Validation des premières simulations MRCC5 pilotées par des réanalyses sur le Québec* (Internal report No. 19). Montréal, Canada: Ouranos Inc.
- Bourgouin, P. (2000). A method to determine precipitation types. *Weather and Forecasting*, 15, 583–592.
- Carrera, M. L., Gyakum, J. R., & Lin, C. A. (2009). Observational study of wind channelling within the St. Lawrence River Valley. *Journal of Applied Meteorology and Climatology*, 48, 2341–2361.
- Cheng, C. S., Auld, H., Li, G., Klaassen, J., & Li, Q. (2007). Possible impacts of climate change on freezing rain in south-central Canada using down-scaled future climate scenarios. *Natural Hazards and Earth System Science*, 7, 71–87.
- Cheng, C. S., Auld, H., Li, G., Klaassen, J., Tugwood, B., & Li, Q. (2004). An automated synoptic typing procedure to predict freezing rain: An application to Ottawa, Ontario, Canada. *Weather and Forecasting*, 19, 751–768.
- Cortinas Jr, J. V., Bernstein, B. C., Robbins, C. C., & Strapp, J. W. (2004). An analysis of freezing rain, freezing drizzle, and ice pellets across the United States and Canada: 1976–90. *Weather and Forecasting*, 19, 377–390.
- Côté, J., Gravel, S., Méthot, A., Patoine, A., Roch, M., & Staniforth, A. (1998). The operational CMC-MRB global environmental multiscale (GEM) model. Part I: Design considerations and formulation. *Monthly Weather Review*, 126, 1373–1395.
- Davies, H. (1976). A lateral boundary formulation for multi-level prediction models. *Quarterly Journal of the Royal Meteorological Society*, 102 (432), 405–418.
- Dee, D., Uppala, S., Simmons, A., Berrisford, P., Poli, P., Kobayashi, S., ... Vitart, F. (2011). The ERA-Interim reanalysis: Configuration and performance of the data assimilation system. *Quarterly Journal of the Royal Meteorological Society*, 137, 553–597.
- DeGaetano, A. T. (2000). Climatic perspective and impacts of the 1998 northern New York and New England ice storm. *Bulletin of the American Meteorological Society*, 81, 237–254.
- Delage, Y. (1997). Parameterising sub-grid scale vertical transport in atmospheric models under statically stable conditions. *Boundary-Layer Meteorology*, 82(1), 23–48.
- Delage, Y., & Girard, C. (1992). Stability functions correct at the free convection limit and consistent for both the surface and Ekman layers. *Boundary-Layer Meteorology*, 58(1–2), 19–31.
- Environment Canada. (2015). *MANOBS: manual of surface weather observations*. Retrieved from https://www.ec.gc.ca/manobs/73BC3152-E142-4AEE-AC7D-CF30DAFF9F70/MANOBS_7E-A19_Eng_web.pdf
- Groisman, P. Y., Bulygina, O. N., Yin, X., Vose, R. S., Gulev, S. K., Hanssen-Bauer, I., & Førland, E. (2016). Recent changes in the frequency of freezing precipitation in North America and northern Eurasia. *Environmental Research Letters*, 11(4), 045007.

- Gyakum, J. R., & Roebber, P. J. (2001). The 1998 ice storm - Analysis of a planetary-scale event. *Monthly Weather Review*, 129, 2983–2997.
- Henson, W., & Stewart, R. (2007). Severity and return periods of icing events in the Montreal area. *Atmospheric Research*, 84, 242–249.
- Henson, W., Stewart, R., Kochtubajda, B., & Thériault, J. (2011). The 1998 ice storm: Local flow fields and linkages to precipitation. *Atmospheric Research*, 101(4), 852–862.
- Institute for Catastrophic Loss Reduction. (2013). *15 years later: Ice storm revisited*. Retrieved from <http://www.iclr.org/resourcecentre/icestorm98mainpage.html>
- Kain, J. S., & Fritsch, J. M. (1990). A one-dimensional entraining/detraining plume model and its application in convective parameterization. *Journal of the Atmospheric Sciences*, 47, 2784–2802.
- Klima, K., & Morgan, M. G. (2015). Ice storm frequencies in a warmer climate. *Climatic Change*, 133(2), 209–222.
- Kuo, H.-L. (1965). On formation and intensification of tropical cyclones through latent heat release by cumulus convection. *Journal of the Atmospheric Sciences*, 22(1), 40–63.
- Lackmann, G. M., Keeter, K., Lee, L. G., & Ek, M. B. (2002). Model representation of freezing and melting precipitation: Implications for winter weather forecasting. *Weather and Forecasting*, 17(5), 1016–1033.
- Lambert, S. J., & Hansen, B. K. (2011). Simulated changes in the freezing rain climatology of North America under global warming using a coupled climate model. *Atmosphere-Ocean*, 49(3), 289–295.
- Laprise, R. (1992). The Euler equations of motion with hydrostatic pressure as independent variable. *Monthly Weather Review*, 120, 197–207.
- Li, J., & Barker, H. (2005). A radiation algorithm with correlated-k distribution. Part I: Local thermal equilibrium. *Journal of the Atmospheric Sciences*, 62(2), 286–309.
- Lucas-Picher, P., Laprise, R., & Winger, K. (2016). Evidence of added value in North American regional climate model simulations using ever-increasing horizontal resolutions. *Climate Dynamics*. Advance online publication. doi:10.1007/s00382-016-3227-z
- Martynov, A., Laprise, R., Sushama, L., Winger, K., Šeparović, L., & Dugas, B. (2013). Reanalysis-driven climate simulation over CORDEX North America domain using the Canadian Regional Climate Model, version 5: Model performance evaluation. *Climate Dynamics*, 41(11–12), 2973–3005.
- McFarlane, N. (1987). The effect of orographically excited gravity wave drag on the general circulation of the lower stratosphere and troposphere. *Journal of the Atmospheric Sciences*, 44(14), 1775–1800.
- McKay, G. A., & Thompson, H. A. (1969). Estimating the hazard of ice accretion in Canada from climatological data. *Journal of Applied Meteorology*, 8(6), 927–935.
- McTaggart-Cowan, R., & Zadra, A. (2015). Representing Richardson number hysteresis in the NWP boundary layer. *Monthly Weather Review*, 143(4), 1232–1258.
- Milton, J., & Bourque, A. (1999). *A climatological account of the January 1998 ice storm in Quebec* (Tech. Rep. No. CES-Q99-01). Quebec: Environment Canada.
- Razy, A., Milrad, S. M., Atallah, E. H., & Gyakum, J. R. (2012). Synoptic-scale environments conducive to orographic impacts on cold-season surface wind regimes at Montreal, Quebec. *Journal of Applied Meteorology and Climatology*, 51, 598–616.
- Regan, M. (1998). Canadian ice storm 1998. *WMO Bulletin*, 47, 250–256.
- Ressler, G. M., Milrad, S. M., Atallah, E. H., & Gyakum, J. R. (2012). Synoptic-scale analysis of freezing rain events in Montreal, Quebec, Canada. *Weather and Forecasting*, 27, 362–378.
- Roebber, P. J., & Gyakum, J. R. (2003). Orographic influences on the mesoscale structure of the 1998 ice storm. *Monthly Weather Review*, 131, 27–50.
- Šeparović, L., Alexandru, A., Laprise, R., Martynov, A., Sushama, L., Winger, K., ... Valin, M. (2013). Present climate and climate change over North America as simulated by the fifth-generation Canadian Regional Climate Model. *Climate Dynamics*, 41(11–12), 3167–3201.
- Stuart, R. A., & Isaac, G. A. (1999). Freezing precipitation in Canada. *Atmosphere-Ocean*, 37(1), 87–102.
- Sundquist, H. (1978). A parameterization scheme for non-convective condensation including prediction of cloud water content. *Quarterly Journal of the Royal Meteorological Society*, 104, 677–690.
- Thériault, J. M., & Stewart, R. E. (2010). A parameterization of the microphysical processes forming many types of winter precipitation. *Journal of the Atmospheric Sciences*, 67, 1492–1508.
- Thériault, J. M., Stewart, R. E., & Henson, W. (2010). On the dependence of winter precipitation types on temperature, precipitation rate, and associated features. *Journal of Applied Meteorology and Climatology*, 49, 1429–1442.
- Verseghy, D. L. (1991). CLASS—A Canadian land surface scheme for GCMs. I. Soil model. *International Journal of Climatology*, 11(2), 111–133.
- Verseghy, D. L. (2009). CLASS—The Canadian Land Surface Scheme (version 3.4) technical documentation (version 1.1), Environment Canada. Climate Research Division, Science and Technology Branch, Downsview, Ontario, Canada.
- Yeh, K.-S., Côté, J., Gravel, S., Méthot, A., Patoine, A., Roch, M., & Staniforth, A. (2002). The CMC-MRB global environmental multiscale (GEM) model. Part III: Nonhydrostatic formulation. *Monthly Weather Review*, 130(2), 339–356.
- Zadra, A., McTaggart-Cowan, R., Vaillancourt, P., Roch, M., Bélair, S., & Leduc, A. (2014). *Improvements to the Global Deterministic Prediction System (GDPS)(from version 2.2.2 to 3.0.0), and related changes to the Regional Deterministic Prediction System (RDPS)(from version 3.0.0 to 3.1.0)* (Tech. Rep.). Canadian Meteorological Centre. Retrieved from http://collaboration.cmc.ec.gc.ca/cmc/CMOI/productguide/docs/lib/op_systems/doc_opchanges/technote_gdps30020130213e.pdf
- Zadra, A., Roch, M., Laroche, S., & Charron, M. (2003). The subgrid-scale orographic blocking parametrization of the GEM Model. *Atmosphere-Ocean*, 41, 155–170.
- Zerr, R. J. (1997). Freezing rain: An observational and theoretical study. *Journal of Applied Meteorology*, 36, 1647–1661.